RESEARCH   **Open Access**

SPH propagation back-analysis of Baishuihe landslide in south-western China

Anika Braun[1*], Xueliang Wang[1], Stefano Petrosino[2] and Sabatino Cuomo[2]

Abstract

Background: Landslides and landslide dams are a major natural hazard causing high socioeconomic risk in inhabited mountainous areas. This is also true for vast parts of south-western China, which are highly prone to slope failures due to several factors, such as a humid climate with high precipitation in the summer months, geological predisposing factors with highly weathered sedimentary rocks and a high seismicity. In order to assess possible run-out distances and the potential of landslides to block rivers, it is crucial to understand which factors influence landslide propagation and how they can be quantified. Since it is often difficult or impossible to measure related geotechnical parameters in the field, their back analysis with a numerical modelling approach can be useful. In this study a numerical modelling analysis was implemented for the case of a complex landslide in south-western China, which transformed into a debris flow and blocked the river and a major road after heavy rainfall. For this purpose a quasi-3D smoothed particle hydrodynamics (SPH) model that can account for geotechnical slope parameters, run-out distance, velocities, and deposition heights was used. Based on field observations regarding initial landslide volume and final deposition volume, height, and length, the mechanical properties of the landslide were estimated in a back-analysis.

Results: Through stepwise parameter optimisation the best reconstruction of the observed deposition phenomena could be achieved considering an initial landslide volume of about 0.5 million cubic meters, a triggering height of 15 m, an height of the water table equal to half the soil thickness, initial pore water pressures of about 0.6 of the liquefaction value, and non-negligible bed entrainment, which resulted in a deposition with a volume of about one million cubic meters, a length of 615 m and a mean height of 11 m. Compared to models with other parameter combinations, here the total error was minimal, while the final deposition dimensions were only slightly overestimated with regard to the observations in the field.

Conclusions: The paper outlines the potential for quantitatively interpreting the field evidence for the propagation of a complex flow-like landslide and related cascading processes, such as landslide damming. However, the analysis should take into account multiple features of the whole processes, such as the initial conditions at the landslide source area, the propagation pattern, the total volume mobilised, and the deposition characteristics. By doing so, the estimated model parameters can be implemented in future studies for the forward modelling of events at the same site, or other sites along this slope, in order to assess the potential of future river blockings through landslide deposits.

Keywords: Modelling, Propagation, Entrainment, Pore water pressure, Deposition

---

* Correspondence: anika.braun@rwth-aachen.de
[1]Chinese Academy of Sciences, Institute of Geology and Geophysics, No. 19 Beitucheng Western Road, 100029 Beijing, China
Full list of author information is available at the end of the article

Braun *et al. Geoenvironmental Disasters* (2017) 4:2

Page 2 of 10

Background

Landslides, and particularly debris flows, are a major natural hazard causing high socioeconomic risk in inhabited mountainous areas. The flows of saturated non-plastic debris usually occur in established drainage channels at rapid to extremely rapid velocities with high peak discharges and long travel distances, which give them a high destructive potential (Hungr et al. 2001). Dams formed by landslide deposits are a common phenomenon that can cause upstream flooding conditions as well as outburst floods during uncontrolled dam breaks (Costa and Schuster 1988; Korup 2002), affecting the most vulnerable areas in mountainous regions, the valleys. In order to protect these areas, by means of adapted land-use planning and implementation of mitigation measures, the modelling of debris flow run-out distances, deposition heights and velocities in site-specific studies is an important tool for the identification of hazardous zones, assessing the potential for landslide dam formation, planning of engineering measures, and the quantification of debris flow intensities as a first step towards a hazard and risk assessment (Corominas et al. 2014).

Methods for the modelling of landslide run-out are usually empirical or rational. While empirical models rely on the establishment of a relationship between landslide run-out and geometrical or morphological characteristics observed in the field (Corominas et al. 2014), rational methods are based on mathematical models, usually expressed by partial differential equations that can be solved analytically or numerically (Pastor et al. 2014), and provide a better means for the quantification of relevant parameters. Numerical modelling is particularly useful for the estimation of parameters that cannot easily be measured in the field or in experiments, such as rheological parameters of the sliding mass and pore water pressures, through back analysis (Cascini et al. 2014). Rational models can further be classified into discrete and continuum based models. In discrete models single blocks or a number of blocks or particles, their impact with the topographic surface and contacts with each other are considered. According to Pastor et al. (2014) they are rather suited for the modelling of debris avalanches than flow processes. Continuum models are based on continuum mechanics and allow the coupling of mechanical, hydraulic and thermo-mechanical behaviour. The classical approaches in geotechnical engineering are velocity–pressure (Biot-Zienkiewicz) models, where the velocities of soil particles and the pore pressures of the interstitial fluids are considered (Pastor et al. 2014). These models are usually formulated in three-dimensional (3D) space, but can be further simplified by depth integration, resulting in two-dimensional (2D) discretization (Pastor et al. 2009). Examples of studies have been provided in recent years and it is worth mentioning the modelling of debris flows (Cascini et al., 2014, 2016) and debris avalanches (Cuomo et al., 2014, 2016).

For the numerical solution, discretization of the model in time and space is required. Here Eulerian methods, based on grids fixed in space, and Lagrangian methods, where discrete points move with the fluid, allowing the separation of meshes for terrain and fluid, can be distinguished (Pastor et al. 2014). Especially for the modelling of phenomena associated with large deformations, free surfaces, deformable boundaries, moving interfaces, and crack propagation the use of meshes can lead to numerical difficulties and distortions (Huang and Dai 2014). One promising alternative for Lagrangian discretization is the meshless smoothed particle hydrodynamics (SPH) technique that was originally introduced by Lucy (1977) and Gingold and Monaghan (1977) for astrophysical modelling. The advantages of SPH compared to mesh-based methods are the reduction of computer time and the avoidance of mesh distortions (Pastor et al. 2014; Huang and Dai, 2014). The technique has been implemented for the numerical modelling of landslide propagation, e.g. by Bonet and Rodriguez-Paz (2005), McDougall (2006), and McDougall and Hungr (2004). Later it has been introduced to the hydro-mechanically coupled modelling of landslides of the flow type by Pastor et al. (2009) and successfully applied to case studies e.g. by Cascini et al. (2014) and Pastor et al. (2014). More extensive literature reviews about the numerical modelling of landslide run-out, especially with SPH techniques, are for instance provided in Corominas et al. (2014), Huang and Dai (2014), or Pastor et al. (2014).

Landslides and associated landslide dams are a major concern in many parts of south-western China. Due to several factors, such as a humid climate with high precipitation in the summer months, geological conditions with partially extremely weathered sedimentary rocks, a high seismicity and intensive land-use near rapidly urbanizing areas, the region is highly susceptible to slope failures and the resulting debris availability as well as high rainfall favour the evolution of debris flows. One example is the Baishuihe landslide in Ningnan county, in the southeast of Sichuan province. It was activated twice in the year 2012 after heavy rainfall, and transformed into a debris flow, which left two persons dead and three missing, damaged houses, and blocked the main road and the river, resulting in upstream flooding. The threat of future events persists with the source zone still being unstable.

The objective of the present study is to model the run-out distance, velocity and deposition heights of the Baishuihe debris flow in order to assess the potential of future damage and formation of landslide dams. A coupled hydro-mechanical depth-integrated SPH approach was employed to numerically model the propagation of the debris flow. Because limited amount of field data was available, the relevant geotechnical parameters were estimated by back-analysis of the occurred event. The results of the

Braun et al. Geoenvironmental Disasters (2017) 4:2

Page 3 of 10

analysis can later be used for the prediction of future events at this specific site or other similar sites.

Methods

SPH model

The numerical analysis of debris flow propagation and landslide dam formation into the river was performed through the "GeoFlow_SPH" model. This is a depth-integrated hydro-mechanically coupled model proposed by Pastor et al. (2009), based on the fundamental contributions of Hutchinson (1986) and Pastor et al. (2002), which schematizes the propagating mass as a mixture of a solid skeleton and water completely saturating the voids. The unknowns are the velocity of the soil skeleton (v) and the basal pore water pressure (p_w^b). Both variables are defined as the sum of two components related to: i) propagation, and ii) consolidation along the normal direction to the ground surface.

Pastor et al. (2009) discuss the governing equations: i) balance of mass of the mixture – propagating along the slope and increasing due to bed entrainment – combined to the balance of linear momentum of pore water, ii) the balance of linear momentum of the mixture, iii) a kinematic relation between the deformation-rate tensor and velocity field, iv) rheological equation relating the soil-stress tensor to the deformation-rate tensor. Further details are also provided by Pastor et al. (2014), Cascini et al. (2014), and Cuomo et al. (2014).

Particularly, the time-space variations of pore water pressures play a major role in landslide dynamics. Adequate simulation of pore water pressures still poses challenging tasks and a recent discussion was provided by Cuomo (2014) as far as landslide initiation, transformation from slide to flow, landslide propagation, and deposition. In the model here used, the vertical distribution of pore water pressure is approximated using a quarter cosinus shape function, with a zero value at the surface and zero gradient at the basal surface (Pastor et al., 2009). The reason is that consolidation being ruled by a parabolic equation, shorter wavelengths are dissipated very fast, and from the limitation to a single Fourier component, the time-evolution of the basal pore water pressure (p_w^b) is given by Eq. 1, where c_v is the consolidation coefficient:

$$\frac{dp_w^b}{dt} = \frac{\pi^2}{4h^2} c_v p_w^b \qquad (1)$$

As for the rheological model, in the case of a pure frictional mass, the basal tangential stress is given by Eq. 2:

$$\tau_b = -\left((1-n)(\rho_s - \rho_w)g \cdot h \cdot \tan\phi_b - p_w^b\right) \cdot \text{sgn}(\overline{v}) \qquad (2)$$

where τ_b is the basal shear stress, n is the soil porosity, ρ_s is the solid grain density, ρ_w is the water density, g is the gravity acceleration, h is the mobilized soil depth, ϕ_b is the basal friction angle, p_w^b is the basal pore water pressure, sgn is the sign function and $\overline{v}$ is the depth-averaged flow velocity. The initial pore water pressure is taken into account through the relative height of the water, h_w^{rel}, which is the ratio of the height of the water table to the soil thickness, and the relative pressure of the water p_w^{rel}, that is to say the ratio of pore-water pressure to liquefaction pressure. Estimates of both parameters can be obtained from the analysis of the triggering stage, and they play an important role in the propagation stage of a flow-like landslide (Cuomo et al., 2014). An overview of rheological parameters used in previous studies is provided in Table 1.

Bed entrainment is also considered in the model, i.e. increase of landslide volume due to the inclusion of soil, debris and trees uprooted from the ground surface during the flow propagation. Bed entrainment has been formerly documented as an important process either for debris flows (Cascini et al., 2014) or debris avalanches (Cuomo et al., 2014). Because of bed entrainment, the elevation of ground surface (z) diminishes, and its time

Table 1 Rheological parameters used in previous studies.

Case	$\tan\varphi_b$ (–)	h_w^{rel} (–)	p_w^{rel} (–)	c_v (m^{2}s^{-1})	K (–)	E_r (m^{-1})	Reference
DF	0.4	0.25	1.0	1.1×10^{-2}	-	-	Pastor et al. (2009)
DF	0.35 - 0.40	0.4	1.0	1.0×10^{-2}	-	4.0×10^{-4}	Cascini et al. (2012)
DA	0.40	0.25	1.0	1.1×10^{-2}	-	1.2×10^{-3} - 8.2×10^{-3}	Cascini et al. (2013)
DA	0.35	0.40	1.0	1.0×10^{-2}	-	8.2×10^{-3}	Cuomo et al. (2014)
DA	0.41	0.25	1.0	1.0×10^{-2}	-	4.0×10^{-3}	Cuomo et al. (2014)
DA	0.15 - 0.35	0.40	1.0	1.0×10^{-2}	-	4.0×10^{-3}	Cuomo et al. (2014)
DA	0.34	0.4	1.0	1.0×10^{-2}	0.019	-	Cuomo et al. (2016)
DA	0.4	0.25	1.0	1.0×10^{-2}	0.007	-	Cuomo et al. (2016)
DA	0.4	0.4	1.0	1.0×10^{-2}	0.007	-	Cuomo et al. (2016)

DA Debris Avalanches; DF Debris Flows; φ_b basal friction angle, h_w^{rel} relative water height; p_w^{rel}; ratio of pore water pressure to liquefaction pressure; c_v consolidation factor; K empirical parameter for the bed entrainment law of Blanc et al. (2011); E_r: erosion coefficient of Hungr et al. (2005)

Braun *et al. Geoenvironmental Disasters* (2017) 4:2

Page 4 of 10

derivative can be computed based on different so-called "erosion" models, providing empirical or physically based equations for the entrainment rate (e_r). Pirulli and Pastor (2012) and Cascini et al. (2014) provide comprehensive reviews of the entrainment models available in the literature. Here, the formulation proposed by Blanc (2008) and Blanc et al. (2011) is used:

$$\frac{\partial z}{\partial t} = -e_r = -h \cdot v \cdot K \cdot (\tan\theta)^{2.5} \tag{3}$$

where v is the flow velocity, h the propagation height, θ is the slope angle, K is an empirical parameter to be calibrated, and the exponent equal to 2.5 is purely empirical and results from the analysis of experimental data (Blanc, 2008).

The equations are reduced from 3D to a quasi-3D formulation through a depth integration approximation, which is suitable for flow-like landslides because of a low ratio of the soil thickness to the landslide length. This quasi-3D depth-integrated model is both accurate (Cascini et al., 2014; 2016; Cuomo et al., 2014; 2016) and less time-consuming than a fully 3D model.

The SPH method is used to discretise the propagating mass into a set of moving "particles". It allows using a set of ordinary differential equations, while the information such as the unknowns and their derivatives are linked to the particles. The accuracy of the numerical solution and the level of approximation for engineering purposes depend on how the nodes are spaced and on the detail of the digital terrain model (DTM), as shown by Pastor et al. (2012) and Cuomo et al. (2013).

The "GeoFlow_SPH" model was recently used for the back-analysis of the propagation and bifurcation of the above mentioned Tsing Shan debris flow, which occurred in 2000 in Hong Kong (Pastor et al., 2014), and for simulating the interplay of rheology and entrainment during the inception of debris avalanches (Cuomo et al., 2014). Similarly as in both these papers, the frictional rheology is here used because it is a reasonable and effective schematization for mixtures of coarse-grained soils saturated with water. Compared to other models from the literature (e.g. McDougall and Hungr, 2004), the GeoFlow_SPH model has the principal merit to explicitly introduce the hydro-mechanical coupling between the solid skeleton and interstitial (pore water) pressure, the latter one being variable within space and time.

Case study
Setting
The study area is located in Ningnan county in the south of Sichuan province in south-western China (Fig. 1). The climate in the region can be characterized as warm temperate with dry. The mean annual precipitation is 1025 mm, whereas more than 70% of the rainfall occurs during the rainy season between June and September. Ningnan county is located in an almost N-S trending mountain chain at the south-western boundary of the Sichuan basin and the south-eastern margin of the Tibetan Plateau, which reaches peaks of up to 4790 m.

The local geology is characterized by complicated tectonic transformations. According to Deng et al. (2014) the area was located at a continental margin from Paleozoic to Mesozoic times, during which continental flood basalts
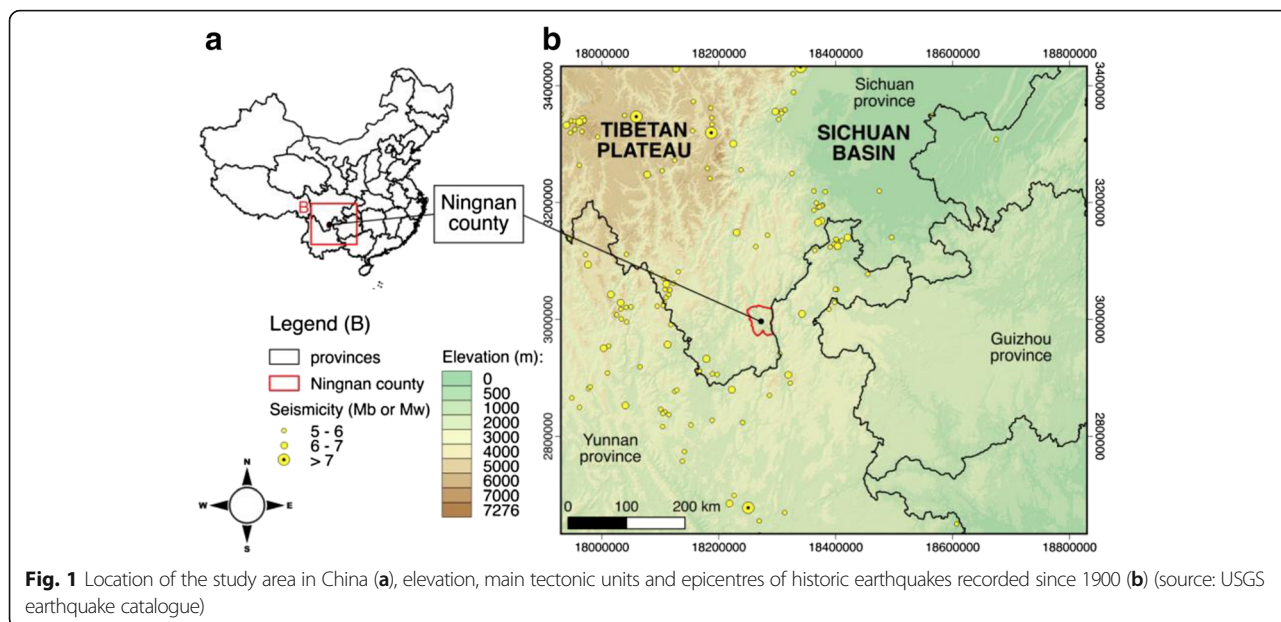

Fig. 1 Location of the study area in China (**a**), elevation, main tectonic units and epicentres of historic earthquakes recorded since 1900 (**b**) (source: USGS earthquake catalogue)

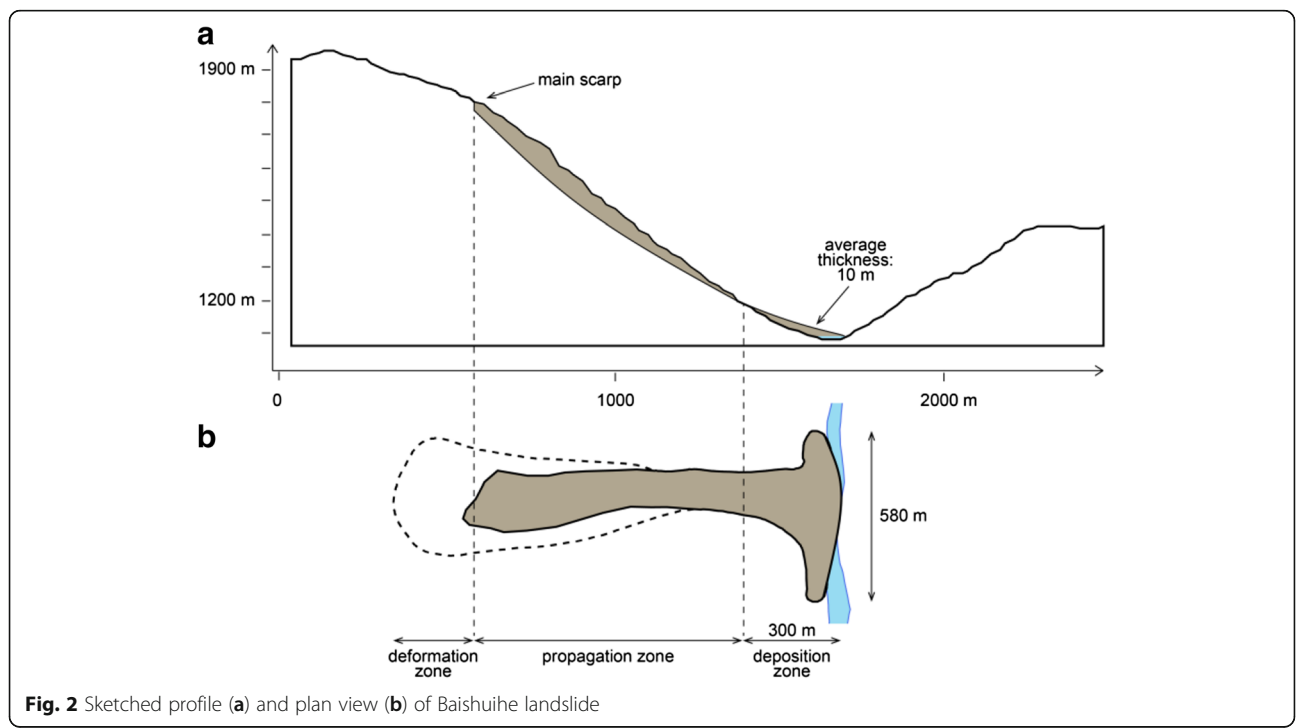Braun *et al. Geoenvironmental Disasters* (2017) 4:2

Page 5 of 10

were deposited in Permian, and marine clastic-carbonate sequences from Silurian to Triassic times. It transformed into a collisional orogeny during Late Triassic and Cenozoic times with the deposition of terrestrial fluvial and lacustrine red bed facies. According to these sedimentation milieus the geology in Ningnan county is characterized by different formations of limestone, dolomite, mudstone, sandstone, and interbedded formations of those lithologies, that were deposited from the Sinian throughout the Cambrian, Ordovician, Silurian and Devonian times as well as from Permian to Jurassic times. Basalts were deposited during the Permian, which crop out in the north and the east of the study area. Moreover there are local deposits of loose Quaternary sediments. Basically, south-western China experiences a relatively high seismic activity, however, in the vicinity of Ningnan county only few significant earthquakes occurred during the last century (Fig. 1), which is why rainfall is believed to be the main trigger of landslides here.

Landslide characteristics and evolution

Baishuihe landslide, located in the north of Ningnan county at 27.296283 N, 102.566979 E, is a complex landslide that transformed into a small debris flow. According to the local villagers the development of deformation and cracking phenomena in the source area started in 2006. In 2012 two significant failures occurred. The first event took place on June 28, when probably 20 slumps transformed into a debris flow after heavy rainfall, resulting in a blockage of the main road at the foot of the slope. Then, on August 16, a second failure occurred, when after high

cumulative rainfall several large scaled slumps transformed into a debris flow again, causing two fatalities, three persons missing, the damage of 38 houses and the blockage of the river, which resulted in a 4 m water level rise upstream. Intermittent small and medium scaled sliding was reported in the aftermath of the events. Moreover, new larger events occurred in September 2015 and May 2016 after heavy rainfall, that were now channelised by mitigation structures put into place.

The landslide can be divided into three zones, the source area, a debris flow propagation area, and the deposition area (Figs. 2 and 4). The source area is located at an elevation between 2100 m and 1615 m, consisting of zones with different degrees of deformation. It is characterized by a distinct main scarp in the front and several other major cracks, shear and tensile failures in the area above. Right after the main event occurred, the deformation area was estimated to stretch over an area of 250 × 400 m, with a thickness between 15 m and 26.7 m, an average thickness of 18 m, and an estimated volume of 1,760,000 m^3, whereas a volume of 540,000 m^3 was given for the main failure. The debris flow propagation zone stretches between an elevation of 1820 m and 1150 m with an approximated area of 140 × 1070 m, an average thickness of 4 m, and a volume of 600,000 m^3. The T-shaped debris accumulation fan is located at the foot of the hill, stretching over an area of 580 × 300 m, with an average thickness of 10 m, and an approximated volume of 870,000 m^3. Due to the narrow shape of the valley with steep slopes characterised by slope angles between 30° and

Fig. 2 Sketched profile (**a**) and plan view (**b**) of Baishuihe landslide

Braun *et al. Geoenvironmental Disasters* (2017) 4:2

Page 6 of 10

50° the run-out of the debris flow was limited by the opposite slope.

These observations of the deposition area dimensions could be verified to a certain degree in a field campaign in 2016. A river bank collapse on the opposite site of the river indicates the landslide run-out of the main event, with a little run-up of material on the opposite slope, which is however very steep and subject to river erosion. A fresh river bank collapse some meters further to the south marks the run-out of the recent event that occurred in May 2016, as can be seen in the drone photo in Fig. 3. The main deformation area and landslide scarp are located within an Ordovician formation consisting of rather soft sandstone/mudstone interlayers that are heavily weathered and fractured, while the debris flow propagation and deposition zones are located within a relatively hard Cambrian dolomite formation (Fig. 4).

The geological formations are dipping into the same direction as the slope, so dip slope or anaclinical conditions apply. According to field observations and laboratory analyses, the sliding material is mainly composed of rocks and debris from the interlayered sandstone/mudstone strata, with 55% to 70% gravel (2 cm to 8 cm), 15% stones (20 cm to 30 cm), sandy soil and occasionally boulders with a size of up to 3 m. However, the occurrence of material from the dolomite strata within the deposited debris indicates that entrainment processes have occurred during the propagation stage of the slide. The shear zone material consists of 55% clayey soil breccia, 20–25% clay and 20–25% silt and sand. The soil breccia has a uniform particle size of 2 to 5 mm and is well sorted.

Results and Discussion

A back analysis was carried out using the above-described "GeoFlow_SPH" model in order to estimate the initial volume (V_{in}) of the landslide and the main mechanical properties. Based on field evidence, the area in front of the main scarp down to an elevation of approximately 1650 m + NN, covering roughly 36,675 m^2, was assumed as the main source of mobilized material. During the simulations the height of this area was varied between 15 m, 20 m, and 25 m, resulting in an initial landslide volume of 550,125 m^3, 733,500 m^3, and 916,875 m^3, respectively. The modelling was performed by changing the main mechanical properties, aimed to understand the relevant factors for the case study. The rheological properties of the main cases analysed are provided in Table 2. A DTM with a cell size of 5 m was interpolated from 20 m contour lines and used as input for the modelling.

The interaction of the flow-like landslide with the river water was not included into the modelling. This hypothesis was based on several reasons: i) the landslide volume was huge (>500,000 m3) and the related propagation heights (>15 m) were larger than the water level inside the river (about 3–4 m); ii) the height difference from the crown to deposition area was about 800 m, thus the landside propagated at very high velocity inside the zone where the landslide body interacted with the river; iii) the bottom of the river is somehow flat and longitudinal slope angle of the river is very small (<5°), thus the water impacted by the landslide was able to spread towards both upslope and downslope the river and effects of landslide-river interaction was limited; iv) the field evidence of landslide run-up to the opposite slope clearly indicate that the landslide was able to overcome the river, thus the interaction with the river was not able to stop the landslide.

The modelling results are reported in Fig. 5, in terms of landslide path, final run-out and volume (V_{fin}), and morphometric features like deposit width (L) and mean height (H_{med}). A combination of field data was used to verify the
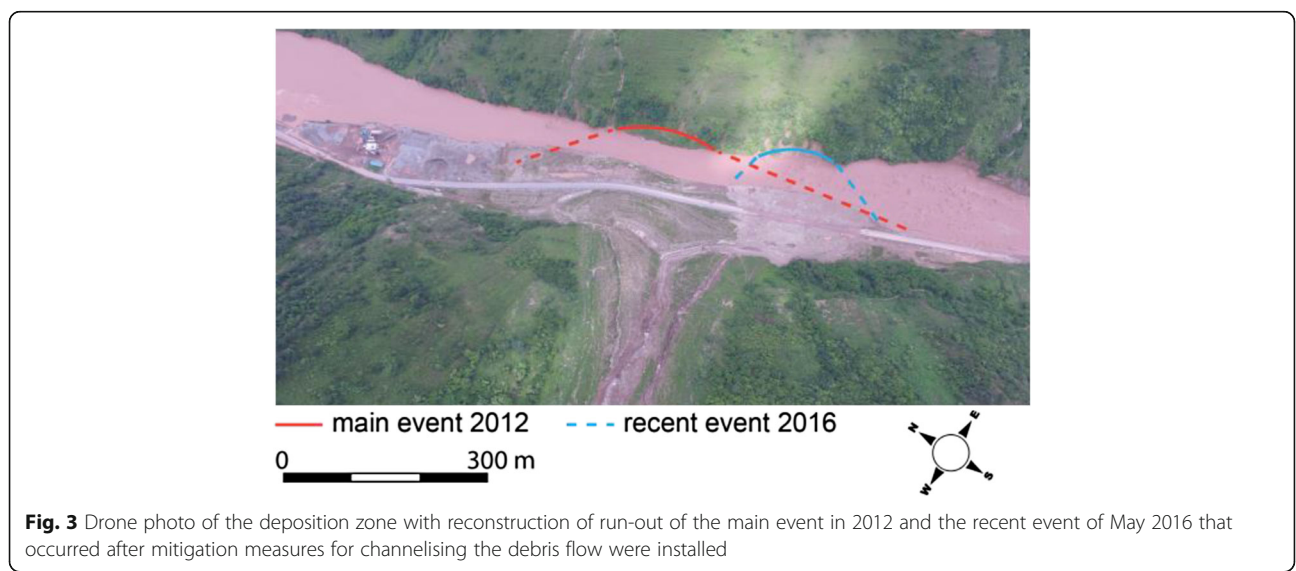

Fig. 3 Drone photo of the deposition zone with reconstruction of run-out of the main event in 2012 and the recent event of May 2016 that occurred after mitigation measures for channelising the debris flow were installed
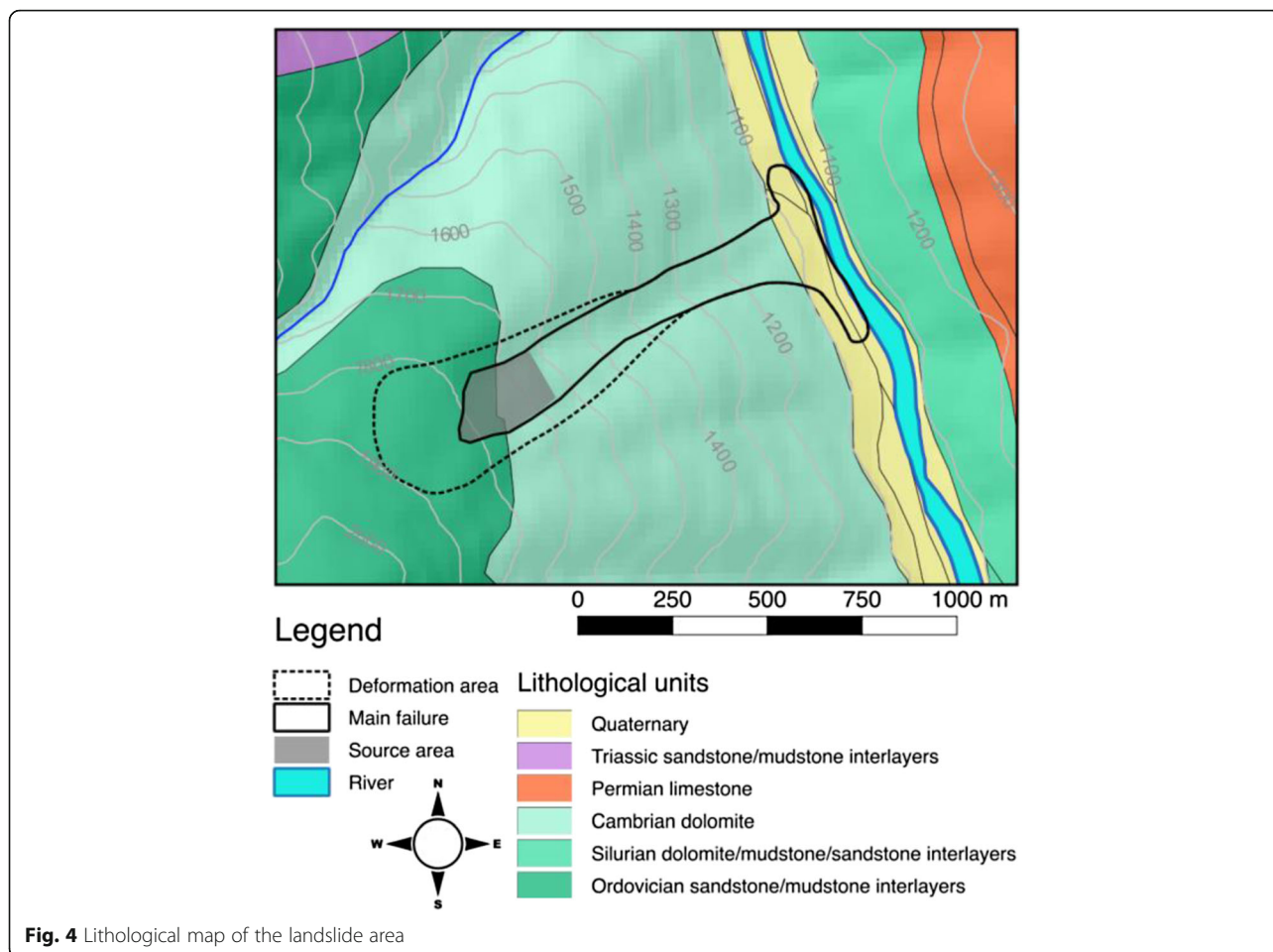
Fig. 4 Lithological map of the landslide area

back analysis results, which included the extent of the landslide source area, the approximated height of soil mobilized, as well as the run-out distance, the shape and main dimensions (width and length) of the landslide deposit, and the average/maximum height of the soil deposit.

First, the final landslide volume was estimated to be 870,000 m^3 according to the field evidence. The landslide run-out is limited due to the narrow shape of the valley and the steep slopes, and thus the width of the landslide deposit in the river direction (580 m) was considered rather than the run-out distance, as it is also an important landslide feature that relates to effective/potential damage and/or post-event mitigation measures. Moreover, the mean height of the deposit (10 m) was considered, since this information may provide an indication of the overall quality of the landslide simulation. In each comparison, the simulated value was normalized to the observed data, whereas a proper simulation would be corresponding to a value close to 1.0. Table 3 and Fig. 6 provide the quality assessment of the modelling results. It must be noted that some simulation cases are relatively

Table 2 Rheological parameters used for modelling

Case	H_{trig} (m)	h_w^{rel} (−)	p_w^{rel} (−)	c_v (m^{2}s^{-1})	K (−)
1	15	0.1	1.0	1.0×10^{-2}	0.007
2	20	0.1	1.0	1.0×10^{-2}	0.007
3	25	0.1	1.0	1.0×10^{-2}	0.007
4	20	0.1	1.0	1.0×10^{-2}	0.019
5	15	0.1	1.0	1.0×10^{-2}	0.019
6	15	0.5	1.0	1.0×10^{-2}	0.007
7	15	0.5	0.8	1.0×10^{-2}	0.007
8	15	0.5	0.6	1.0×10^{-2}	0.007
9	15	0.5	0.6	1.0×10^{-2}	0.006
10	15	0.1	0.8	1.0×10^{-2}	0.007

ρ density of mixture (1300 kg/m^3); H_{trig} height of triggering mass; tan φ_b basal friction angle (0.60); h_w^{rel} relative water height; p_w^{rel} ratio of pore water pressure to liquefaction pressure; c_v consolidation factor, K: empirical parameter for the bed entrainment law of Blanc et al. (2011)
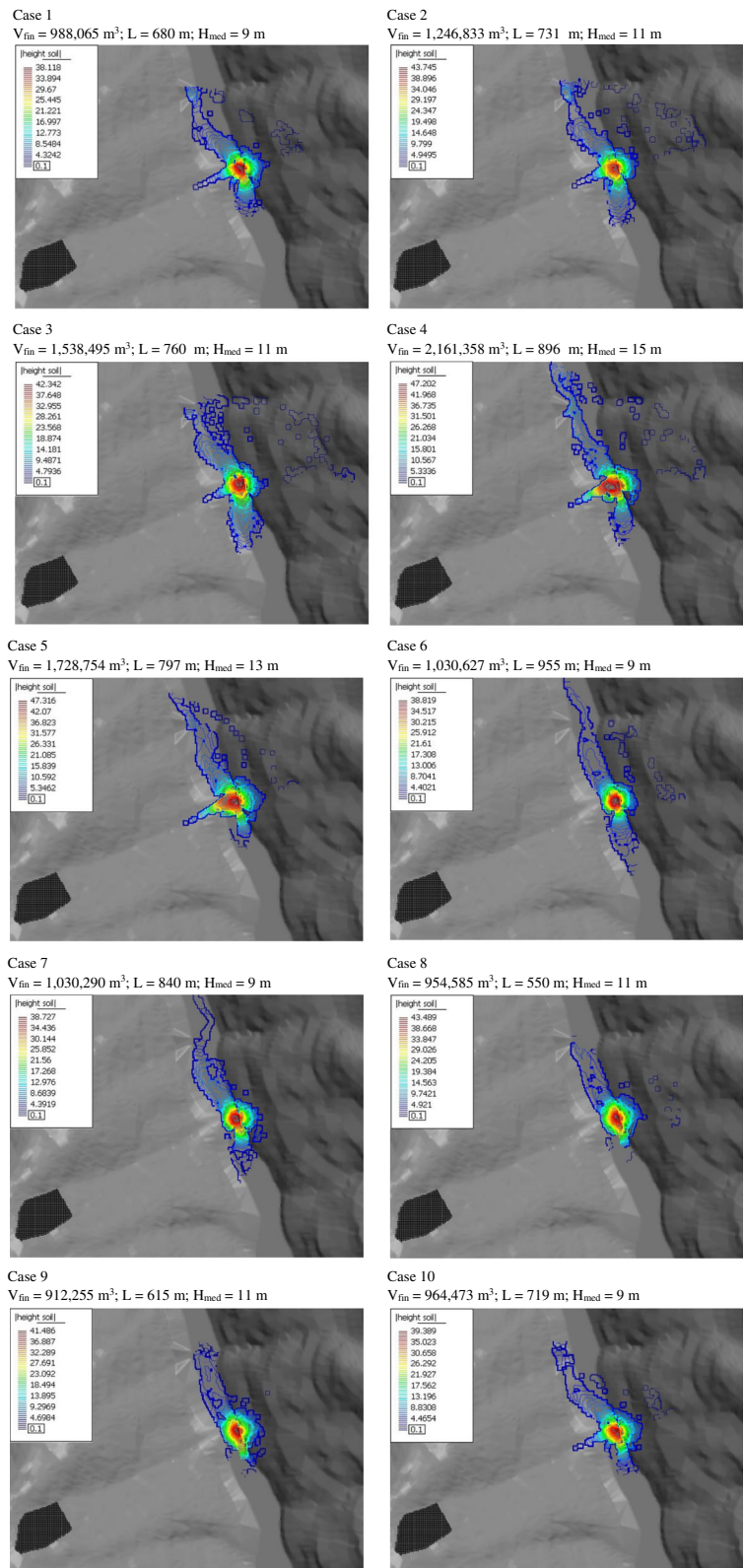
Braun et al. Geoenvironmental Disasters (2017) 4:2

Page 8 of 10

Case 1
$V_{fin} = 988,065$ m^3; L = 680 m; $H_{med} = 9$ m

Case 2
$V_{fin} = 1,246,833$ m^3; L = 731 m; $H_{med} = 11$ m

Case 3
$V_{fin} = 1,538,495$ m^3; L = 760 m; $H_{med} = 11$ m

Case 4
$V_{fin} = 2,161,358$ m^3; L = 896 m; $H_{med} = 15$ m

Case 5
$V_{fin} = 1,728,754$ m^3; L = 797 m; $H_{med} = 13$ m

Case 6
$V_{fin} = 1,030,627$ m^3; L = 955 m; $H_{med} = 9$ m

Case 7
$V_{fin} = 1,030,290$ m^3; L = 840 m; $H_{med} = 9$ m

Case 8
$V_{fin} = 954,585$ m^3; L = 550 m; $H_{med} = 11$ m

Case 9
$V_{fin} = 912,255$ m^3; L = 615 m; $H_{med} = 11$ m

Case 10
$V_{fin} = 964,473$ m^3; L = 719 m; $H_{med} = 9$ m

Fig. 5 Simulated heights of soil deposit (coloured contouring) with the indication of the landslide source area (*black*) for the cases of Table 2

Table 3 Modelling results and comparison with field data

Case	V_{in} (m³)	V_{fin} (m³)	L (m)	H_{med} (m)	V_{norm} (–)	L_{norm} (–)	H_{norm} (–)	RE (–)
1	550125	988065	680	9	1.136	1.172	0.900	0.241
2	733500	1246833	731	11	1.433	1.260	1.100	0.515
3	916875	1538495	760	11	1.768	1.310	1.100	0.835
4	733500	2161358	896	15	2.484	1.545	1.500	1.658
5	550125	1728754	797	13	1.987	1.374	1.300	1.097
6	550125	1030627	955	9	1.185	1.647	0.900	0.680
7	550125	1030290	840	9	1.184	1.448	0.900	0.495
8	550125	954585	550	11	1.097	0.948	1.100	0.149
9	550125	912255	615	11	1.049	1.060	1.100	0.126
10	550125	964473	719	9	1.109	1.240	0.900	0.281

V_{in} initial volume; V_{fin} final volume; L width of deposition zone; H_{med} mean deposition height; L_{norm} normalised width of deposition zone; V_{norm} normalised final volume; RE relative error indicator according to Eq. 4

unrealistic while other cases well match only one or two out of three reference quantities.

A multi-criteria comparison could be useful in such a case. Three indicators (X_i) were used together for computing the mean relative squared error (RE) of the simulated values normalized to the measured values (X_i^s), being 1 corresponding to the optimal solution. Thus, Eq. 4 was used, where the subscript "1" refers to deposit volume, "2" is for deposit width, and "3" for mean deposit height. To the authors' knowledge this type of criterion was not applied before to landslide propagation scenarios.

$$RE = \sqrt{(X_1{}^s - 1)^2 + (X_2{}^s - 1)^2 + (X_3{}^s - 1)^2} \qquad (4)$$

When considering the above-described criteria it turns out firstly that with the increase of the initial volume by raising the triggering height, as well as with a higher bed entrainment parameter K, particularly the final volume of the deposit, but also length and medium height, are clearly overestimated (cases1-5). For this reason, also the pore water terms were changed (cases 6–10). Initially (case 6) only the relative water height (h_w^{rel}) term was increased and this led to acceptable results for the final volume and main height, but to an excessive widening of

the material in the deposition area, Changing at the same time (h_w^{rel}) and also the ratio of pore water pressure to liquefaction pressure (p_w^{rel}) a best fit case was reached (case 9), with the lowest overall error and only slight overestimations of the normalised length, height, and volume criteria. Thus, along the optimisation steps the triggering height was kept at 15 m, while the increase of the relative water height from 0.1 to 0.5, the decrease of the ratio of pore water pressure to liquefaction pressure from 1.0 to 0.6, and the decrease of K from 0.007 to 0.006 resulted in the model with the lowest overall error and only slight overestimations of the normalised length, height, and volume criteria.

More in general, this back-analysis evidences that landslide triggering is reached before full saturation of the soil thickness and far from soil liquefaction condition. The general agreement among field observations of volume, deposition area and height and model results also testifies the quality of the data-set, which includes reliable estimates of the mobilised soil thickness at the landslide source area. In addition, bed entrainment is outlined as a key factor as observed in many catastrophic events in China and other countries.

Conclusions

A numerical modelling analysis with an SPH code has been carried out for a landslide case study in southwestern China in order to back analyse relevant mechanical parameters and better understand the landslide propagation processes. The model parameters were optimised by taking into account field evidence concerning the final landslide volume, the length and height of the deposit, and the final run-out. The best reconstruction of the observed deposition phenomena was achieved with an initial landslide volume of about 0.5×10^6 cubic meters, a triggering height of 15 m, a height of the water table equal to half the soil thickness, initial pore water pressures of about 0.6 of the liquefaction value, and non-negligible bed entrainment, which resulted in a deposition with a volume of about one million of cubic meters. The numerical model provided a good overall match for such a complex phenomenon, as it is found that failure at the landslide
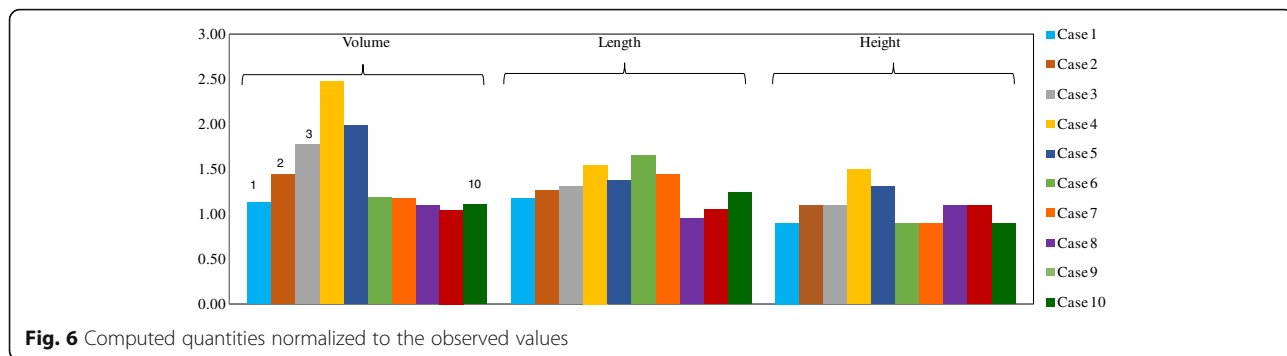
Fig. 6 Computed quantities normalized to the observed values

Braun *et al. Geoenvironmental Disasters* (2017) 4:2

Page 10 of 10

source area occurred before full saturation of the soil thickness and far from soil liquefaction conditions, while bed entrainment is a key factor. The general agreement among field observations of volume, deposition area, and height and model results also testifies the quality of the data-set, which includes reliable estimates of the mobilised soil thickness at the landslide source area. The modelled parameters can be implemented in future studies for the forward modelling of events at the same site, or other sites along this slope, in order to assess the potential of future river blockings through landslide deposits.

Authors' contributions
AB and XW are responsible for the characterization of the case study, the collection and preparation of data and the corresponding passages in the manuscript (sections 1 and 3), while SP and SC are responsible for the numerical modelling analysis and the corresponding passages in the manuscript (sections 2 and 4). The results were discussed and the conclusions drafted jointly by all authors. All authors read and approved the final manuscript.

Competing interests
We hereby declare that none of the authors has any competing financial interests.

Author details
[1]Chinese Academy of Sciences, Institute of Geology and Geophysics, No. 19 Beitucheng Western Road, 100029 Beijing, China. [2]Department of Civil Engineering, University of Salerno, Via Ponte Don Melillo, 84084 Fisciano, Italy.

References
Blanc, T. 2008. *Numerical simulation of debris flows with the 2D SPH depth-integrated model*. Vienna, Austria: Master's thesis, Institute for Mountain Risk Engineering, University of Natural Resources and Applied Life Sciences.

Blanc, T., M. Pastor, M.S.V. Drempetic, and B. Haddad. 2011. Depth integrated modelling of fast landslides propagation. *European Journal of Environmental and Civil Engineering* 15: 51–72.

Bonet, J., and M. Rodriguez-Paz. 2005. A corrected smooth particle hydrodynamics formulation of the shallow-water equations. *Computers and Structures* 83(17): 1396–1410.

Cascini, L., S. Cuomo, M. Pastor, G. Sorbino, and L. Piciullo. 2012. Modeling of propagation and entrainment phenomena for landslides of the flow type: the May 1998 case study. In: E. Eberhardt, C. Froese, K. Turner, and S. Leroueil (eds). Proceedings of the 11th International Symposium on Landslides: Landslides and Engineered Slopes, Banff, Alta., 3–8 June 2012, pp. 1723–1729.

Cascini, L., S. Cuomo, and M. Pastor. 2013. Inception of debris avalanches: Remarks on geomechanical modelling. *Landslides* 10(6): 701–711.

Cascini, L., S. Cuomo, M. Pastor, G. Sorbino, and L. Piciullo. 2014. SPH run-out modelling of channelised landslides of the flow type. *Geomorphology* 214: 502–513.

Cascini, L., S. Cuomo, M. Pastor, and I. Rendina. 2016. SPH-FDM propagation and pore water pressure modelling for debris flows in flume tests. *Engineering Geology* 213: 74–83.

Corominas, J., C. Van Westen, P. Frattini, L. Cascini, J.P. Malet, S. Fotopoulou, F. Catani, M. Van Den Eeckhaut, O. Mavrouli, F. Agliardi, K. Pitilakis, M.G. Winter, M. Pastor, S. Ferlisi, V. Tofani, J. Hervás, and J.T. Smith. 2014. Recommendations for the quantitative analysis of landslide risk. *Bulletin of Engineering Geology and the Environment* 73(2): 209–263.

Costa, J.E., and R.L. Schuster. 1988. The formation and failure of natural dams. *Geological Society of America Bulletin* 100(7): 1054–1068.

Cuomo S. 2014. New Advances and Challenges for Numerical Modeling of Landslides of the Flow Type. Procedia of Earth and Planetary Science, 9: 91–100. DOI: 10.1016/j.proeps.2014.06.004

Cuomo S., M. Pastor, S. Vitale, and L. Cascini. 2013. Improvement of irregular DTM for SPH modelling of flow-like landslides. Proc. of XII International Conference on Computational Plasticity. Fundamentals and Applications (COMPLAS XII), E. Oñate, D.R.J. Owen, D. Peric and B. Suárez (Eds). 3–5 September 2013, Barcelona, Spain. ISBN: 978-84-941531-5-0, pp. 512–521

Cuomo, S., M. Pastor, L. Cascini, and G.C. Castorino. 2014. Interplay of rheology and entrainment in debris avalanches: a numerical study. *Canadian Geotechnical Journal* 51(11): 1318–1330.

Cuomo, S., M. Pastor, V. Capobianco, and L. Cascini. 2016. Modelling the space–time evolution of bed entrainment for flow-like landslides. *Engineering Geology* 212: 10–20.

Deng, B., S.G. Liu, E. Enkelmann, Z.W. Li, T.A. Ehlers, and L. Jansa. 2014. Late Miocene accelerated exhumation of the Daliang Mountains, southeastern margin of the Tibetan Plateau. *International Journal of Earth Sciences* 104(4): 1–21.

Gingold, R.A., and J.J. Monaghan. 1977. Smoothed particle hydrodynamics: theory and application to non-spherical stars. *Monthly Notices of the Royal Astronomical Society* 181(3): 375–389.

Huang, Y., and Z. Dai. 2014. Large deformation and failure simulations for geo-disasters using smoothed particle hydrodynamics method. *Engineering Geology* 168: 86–97.

Hungr, O., S.G. Evans, M.J. Bovis, and J.N. Hutchinson. 2001. A review of the classification of landslides of the flow type. *Environmental & Engineering Geoscience* 7(3): 221–238.

Hungr, O., J. Corominas, and E. Eberhardt, 2005. Estimating landslide motion mechanism, travel distance and velocity. Landslide Risk Management, 99–128

Hutchinson, J.N. 1986. A sliding-consolidation model for flow slides. *Canadian Geotechnical Journal* 23(2): 115–126.

Korup, O. 2002. Recent research on landslide dams – a literature review with special attention to New Zealand. *Progress in Physical Geography* 26: 206–235.

Lucy, L.B. 1977. A numerical approach to the testing of the fission hypothesis. *The Astronomical Journal* 82: 1013–1024.

McDougall, S. 2006. *A new continuum dynamic model for the analysis of extremely rapid landslide motion across complex 3D terrain. PhD thesis*, 253. Vancouver: University of British Columbia.

McDougall, S., and O. Hungr. 2004. A model for the analysis of rapid landslide motion across three-dimensional terrain. *Canadian Geotechnical Journal* 41(6): 1084–1097.

Pastor, M., M. Quecedo, J.A. Fernández-Moredo, M.I. Herreros, E. González, and P. Mira. 2002. Modelling tailings dams and mine waste dumps failures. *Geotechnique* 52: 579–591.

Pastor, M., B. Haddad, G. Sorbino, S. Cuomo, and V. Drempetic. 2009. A depth-integrated, coupled SPH model for flow-like landslides and related phenomena. *International Journal on Numerical Analysis and Methods in Geomechanics* 33(2): 143–172.

Pastor M., and G.B. Crosta. 2012. Landslide runout: Review of analytical/empirical models for subaerial slides, submarine slides and snow avalanche. Numerical modelling. Software tools, material models, validation and benchmarking for selected case studies. Deliverable D1.7 SafeLand Project https://www.ngi.no/downloads/file/5981. Accessed 12 Jan 2017.

Pastor, M., T. Blanc, B. Haddad, S. Petrone, M.S. Morles, V. Drempetic, D. Issler, G.B. Crosta, L. Cascini, G. Sorbino, and S. Cuomo. 2014. Application of a SPH depth-integrated model to landslide run-out analysis. *Landslides* 11(5): 793–812.

Pirulli, M., and M. Pastor. 2012. Numerical study on the entrainment of bed material into rapid landslides. *Geotechnique* 62(11): 959–972.